Nonlinear 3D Spiral Trajectory Tracking of a 3-DOF Helicopter: A Comparative Analysis of SDRE and Successive Approximation Strategies

Ahmet Çağrı Arıcan[1]

Abstract— **This paper compares State-Dependent Riccati Equation (SDRE) and Successive Approximation (SA) controllers for trajectory tracking of a nonlinear three-degree-of-freedom (3-DOF) laboratory helicopter. Both methods provide approximate routes to nonlinear optimal control problems associated with the Hamilton–Jacobi–Bellman (HJB) equation, but they treat the nonlinear dynamics differently. SDRE preserves a state-dependent coefficient representation, whereas SA repeatedly solves locally linearized subproblems. Two simulation scenarios are considered. The first scenario uses step commands with a severe wind-gust interval to verify nominal tracking and disturbance rejection. The second scenario imposes a three-dimensional spiral reference and an asymmetric wind gust to test sustained nonlinear maneuvering. Under the tested conditions, both controllers track the step commands satisfactorily, while the SDRE controller gives smoother responses and lower time-weighted tracking errors in the spiral case. The comparison is quantified using Integral of Time-weighted Absolute Error (ITAE), Integral of Time-weighted Squared Error (ITSE), total quadratic cost, control behavior, and computation time. The results should be interpreted as evidence for the considered benchmark and scenarios rather than as a universal ranking of the two methods.**

I. Introduction

Unmanned aerial vehicle (UAV) control, particularly for three-degree-of-freedom (3-DOF) helicopter platforms, remains a benchmark problem in nonlinear and optimal control because of strong nonlinearities, underactuation, and dynamic coupling among the elevation, pitch, and travel axes. These characteristics make accurate trajectory tracking difficult, especially under aggressive spatial maneuvers and external disturbances.

For nonlinear continuous-time systems, the optimal feedback law is governed by the Hamilton–Jacobi–Bellman (HJB) equation. In practice, however, exact analytical solutions are generally unavailable for systems such as the 3-DOF helicopter. This limitation has motivated the use of suboptimal nonlinear optimal control methods.

SDRE and SA were selected for this comparison because both are Riccati/HJB-related approximate optimal control strategies, yet they use fundamentally different approximations of the same nonlinear plant. This makes it possible to isolate the practical effect of preserving a state-dependent nonlinear representation, as in SDRE, against repeated Jacobian-based local approximation, as in SA, while keeping the same nonlinear benchmark, cost structure, saturation model, and disturbance profile. Fully nonlinear alternatives such as backstepping or exact feedback linearization are important candidates for future comparative studies, but they require a different design framework and are outside the focused scope of this conference paper.

One widely used approach is the State-Dependent Riccati Equation (SDRE) method [1], [2]. In the SDRE framework, the nonlinear system is represented in a state-dependent coefficient (SDC) form, which enables Riccati-based design while preserving the nonlinear dependence of the plant dynamics. On the 3-DOF helicopter benchmark itself, SDRE has been examined through experimental comparison against LQR, sampled-data implementation studies, and moving-region-of-attraction update strategies [3], [4], [5]. Recent SDRE developments further confirm the relevance of the framework in nonlinear control applications, including flight-control implementation, nonlinear estimation/control, and numerical approximation analyses [6], [7], [8], [9], [10]. Additional application-oriented SDRE studies report integral-SDRE multirotor inspection, spacecraft formation control, and underactuated AUV trajectory tracking [11], [12], [13].

Another important methodology is the Successive Approximation (SA) approach, which has been studied extensively since the early development of iterative optimal control techniques [14]. SA-based methods have been applied to nonlinear HJI and HJB problems through iterative and Galerkin-based formulations [15], [16], [17], [18], with applications in bilinear systems, terminal-state-constrained optimization, stochastic systems, kinodynamic planning, and biomedical control [19], [20], [21], [22], [23]. Recent SA-related HJI work also includes robust spacecraft attitude control under actuator misalignments [24]. However, direct SA-based comparisons against SDRE under highly coupled helicopter trajectory-tracking scenarios remain limited.

Motivated by this gap, this paper compares SDRE and SA controllers for a nonlinear 3-DOF helicopter under two scenarios: step tracking and three-dimensional spiral tracking with wind disturbance. The comparison is performed in terms of tracking performance, computational cost, control effort, and the time-weighted metrics ITAE and ITSE.

The main contributions of this paper are summarized as follows:

- A comparative evaluation framework is developed for SDRE and SA controllers on a nonlinear 3-DOF helicopter benchmark.

*This work was not supported by any organization.

[1]Ahmet Çağrı Arıcan is with Faculty of Engineering, Department of Mechanical Engineering, Gazi University, Ankara, Türkiye ahmetcagriarican@gazi.edu.tr

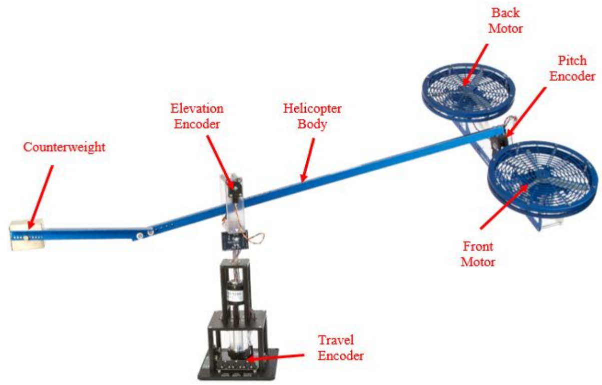

Fig. 1. Experimental 3-DOF helicopter platform.

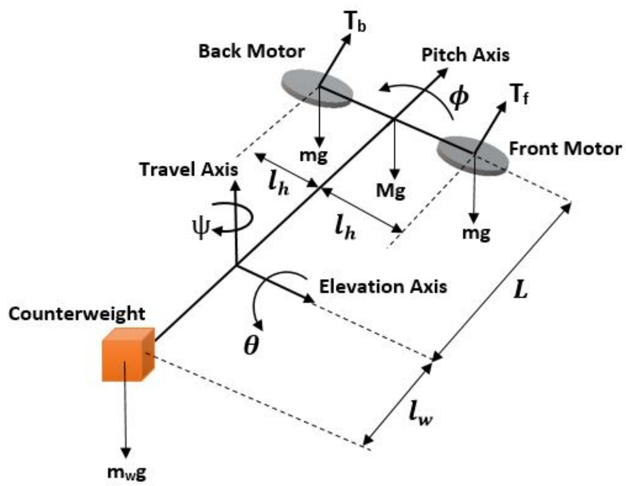

Fig. 2. Free-body diagram of the 3-DOF helicopter benchmark.

- Two operating scenarios are considered: nominal step tracking and a demanding three-dimensional spiral maneuver under asymmetric wind-gust disturbance.
- The controllers are compared quantitatively using computational cost, control effort, ITAE, and ITSE, highlighting the practical advantages of preserving the state-dependent nonlinear structure in SDRE.

II. Mathematical Modeling

The benchmark platform considered in this study is a laboratory 3-DOF helicopter with two propellers and three rotational degrees of freedom: elevation θ, pitch ϕ, and travel ψ. Variants of the same laboratory platform and parameterization have been widely used in earlier SDRE-based helicopter studies, which makes it a suitable benchmark for the present comparison [3], [4], [5]. Although the helicopter can rotate about three axes, it is actuated by only two motor voltages, which makes the system underactuated and strongly coupled. For this reason, the control objective is posed on the elevation and travel coordinates, while the pitch motion is treated as an internal coupled variable that must remain well behaved during the maneuver.

A. Nonlinear Dynamics of the 3-DOF Helicopter

The laboratory 3-DOF helicopter is a nonlinear and strongly coupled underactuated system in which the travel motion is primarily induced through pitch dynamics, as illustrated by the benchmark platform and its free-body representation in Figs. 1 and 2. This coupling leads to a challenging control structure for trajectory tracking and disturbance rejection. The state vector is defined as

TABLE I
Physical Parameters of the 3-DOF Helicopter System

Parameter	Value	Parameter	Value
a_1	0.2517	d_1	0.1011
a_2	0.2105	d_2	0.5040
b_1	0.3290	d_3	1.3400
b_2	1.5664	e_1	6.1600
b_3	16.200	e_2	1.0000
c_1	7.3200	α	4.0000
c_2	1.0000		

$$x = [\theta,\ \phi,\ \psi,\ \dot{\theta},\ \dot{\phi},\ \dot{\psi},\ \tau_{cyc},\ \tau_{coll}]^T,$$

where θ, ϕ, and ψ denote the elevation, pitch, and travel angles, respectively, and τ_{cyc} and τ_{coll} represent the cyclic and collective thrust states. The control input vector is

$$u = [V_f,\ V_b]^T,$$

where V_f and V_b are the voltages applied to the front and back DC motors.

The nonlinear dynamics are expressed in continuous-time state-space form as

$$\dot{x}(t) = f(x) + B_{sys}u(t), \tag{1}$$

with

$$\begin{aligned}
\dot{x}_1 &= x_4,\\
\dot{x}_2 &= x_5,\\
\dot{x}_3 &= x_6,\\
\dot{x}_4 &= -d_1x_4 - d_2\sin(x_1) + d_3x_8\cos(x_2),\\
\dot{x}_5 &= -b_1x_5 - b_2\sin(x_2) - b_3x_7,\\
\dot{x}_6 &= -a_1x_6 - a_2(\alpha x_8 + 1)\sin(x_2),\\
\dot{x}_7 &= -c_1x_7 + \frac{c_2}{2}u_2 - \frac{c_2}{2}u_1,\\
\dot{x}_8 &= -e_1x_8 + \frac{e_2}{2}u_1 + \frac{e_2}{2}u_2.
\end{aligned} \tag{2}$$

Here, a_i, b_i, c_i, d_i, and e_i denote the physical parameters associated with inertia, damping, and thrust-generation dynamics. The numerical values of these parameters are listed in Table I for reproducibility.

B. State-Dependent Coefficient Parameterization

The SDRE approach requires the nonlinear drift term $f(x)$ to be factorized in the state-dependent coefficient form

$$f(x) = A(x)x, \tag{3}$$

so that the nonlinear system can be written as

$$\dot{x}(t) = A(x)x(t) + B_{sys}u(t), \tag{4}$$

where $A(x) \in \mathbb{R}^{8\times 8}$ is a state-dependent system matrix. Since $f(x)$ is continuously differentiable and satisfies $f(0) = 0$, such a factorization exists, although it is not unique.

For the considered helicopter model, the principal nonzero elements of $A(x)$ are given by

$$A_{1,4} = A_{2,5} = A_{3,6} = 1,$$
$$A_{4,1} = -d_2 L(x), \quad A_{4,4} = -d_1, \quad A_{4,8} = d_3 \cos(x_2),$$
$$A_{5,2} = -b_2 M(x), \quad A_{5,5} = -b_1, \quad A_{5,7} = -b_3,$$
$$A_{6,2} = -a_2(\alpha x_8 + 1)M(x), \quad A_{6,6} = -a_1,$$
$$A_{7,7} = -c_1, \quad A_{8,8} = -e_1,$$

where the auxiliary functions

$$L(x) = \frac{\sin(x_1)}{x_1}, \qquad M(x) = \frac{\sin(x_2)}{x_2} \tag{5}$$

are introduced to avoid singularities at the equilibrium point. Using L'Hôpital's rule,

$$\lim_{x_i \to 0} \frac{\sin(x_i)}{x_i} = 1,$$

which ensures that $A(x)$ remains smooth and well defined in a neighborhood of the origin.

III. Controller Synthesis and Theoretical Formulation

To eliminate steady-state tracking errors, the system is augmented with integral error states defined as

$$e_I(t) = \int_0^t \left(C_{aug} x(\tau) - r(\tau)\right) d\tau, \tag{6}$$

where $r(t) = [\theta_{ref}(t), \ \psi_{ref}(t)]^T$ and C_{aug} selects the controlled elevation and travel outputs from the plant state. The augmented state is then written as

$$x_{aug}(t) = [x^T(t) \ e_I^T(t)]^T \in \mathbb{R}^{10}. \tag{7}$$

The control objective is to determine a state-feedback input $u(t)$ that minimizes the infinite-horizon quadratic cost function

$$J = \frac{1}{2} \int_0^\infty \left(x_{aug}^T(t) Q x_{aug}(t) + u^T(t) R u(t)\right) dt, \tag{8}$$

where $Q = Q^T \geq 0$ penalizes state deviations and $R = R^T > 0$ penalizes control effort.

A. SDRE Control Strategy

Within the SDRE framework, the augmented tracking model is represented as

$$\begin{aligned} \dot{x}_{aug}(t) &= \begin{bmatrix} f(x) + B_{sys} u(t) \\ C_{aug} x(t) - r(t) \end{bmatrix} \\ &= A_{aug}(x) x_{aug}(t) + B_{aug} u(t) + E_r r(t), \end{aligned} \tag{9}$$

where $E_r = \begin{bmatrix} 0_{8\times 2} \\ -I_2 \end{bmatrix}$. The reference-dependent term is therefore introduced only through the integral tracking-error dynamics; it is not an additional term in the physical helicopter equations. For the Riccati equation, the feedback gain is obtained from the homogeneous augmented pair $(A_{aug}(x), B_{aug})$, while the reference term acts as an exogenous tracking input in the simulation. The SDRE method computes a state-dependent feedback law by solving the algebraic state-dependent Riccati equation

$$A_{aug}^T P(x) + P(x) A_{aug} - P(x) B_{aug} R^{-1} B_{aug}^T P(x) + Q = 0. \tag{10}$$

The corresponding feedback gain is obtained as

$$K(x) = R^{-1} B_{aug}^T(x) P(x). \tag{11}$$

A standard requirement for the applicability of the SDRE approach is pointwise stabilizability of the pair $(A_{aug}(x), B_{aug}(x))$, together with the corresponding observability condition. In the simulations, the controllability of the augmented system was checked numerically along the state trajectory by evaluating

$$\mathscr{C}(x) = \left[B_{aug}, \ A_{aug} B_{aug}, \ \ldots, \ A_{aug}^9 B_{aug}\right]. \tag{12}$$

This verification supports the existence of a positive-definite Riccati solution throughout the simulated operating region. Since the reference signal is injected only into the integral-error channels, this modeling step does not change the plant dynamics used for stabilizability checks.

Because the SDRE design preserves the state-dependent nonlinear structure of the model, the resulting feedback gain varies continuously with the operating condition. This feature makes the method suitable for the nonlinear flight regimes tested here. Nevertheless, the simulations reported below do not constitute a general proof that SDRE will outperform SA for all references, tunings, or disturbance profiles.

B. Successive Approximation Strategy

Unlike SDRE, the successive approximation (SA) method approaches the nonlinear optimal control problem through a sequence of locally linearized subproblems [25]. Based on Pontryagin's Minimum Principle, the Hamiltonian is defined as

$$\mathscr{H} = \frac{1}{2}\left(x_{aug}^T Q x_{aug} + u^T R u\right) + \lambda^T f_{aug}(x_{aug}, u), \tag{13}$$

where $\lambda(t)$ is the costate vector.

At each iteration, the nonlinear vector field is approximated around the previously computed trajectory $(x^{(k)}, u^{(k)})$ using a first-order Taylor expansion:

$$\begin{aligned} f(x,u) \approx \ & f(x^{(k)}, u^{(k)}) + \left.\frac{\partial f}{\partial x}\right|_{(k)} \Delta x \\ & + \left.\frac{\partial f}{\partial u}\right|_{(k)} \Delta u + \mathscr{O}\left(\|[\Delta x, \Delta u]\|^2\right), \end{aligned} \tag{14}$$

where the higher-order terms are neglected. As a result, the original nonlinear two-point boundary value problem is converted into a sequence of linearized subproblems [26].

In the present implementation, the SA algorithm is applied in a discrete-time marching manner at a sampling rate of 250 Hz. The Jacobian matrices are updated using the state of the previous sampling instant, and the control gain for the current step is computed from this local linear model. This procedure is computationally attractive and straightforward to implement. However, its validity depends on the assumption that the deviation from the linearization point remains sufficiently small between successive steps.

For aggressive three-dimensional maneuvers and in the presence of external wind disturbances, the helicopter states may depart significantly from the local operating point. Under such conditions, the neglected higher-order nonlinear terms become increasingly influential, which can reduce tracking accuracy and may lead to oscillatory closed-loop behavior.

C. Actuator Saturation and Anti-Windup

Since the helicopter is driven by DC motors with finite voltage limits, the commanded control input must satisfy actuator saturation constraints. To generate bounded and smooth inputs, the following hyperbolic tangent saturation law is used:

$$u_{applied} = v_{max} \tanh\left(\frac{u_{cmd}}{v_{max}}\right). \tag{15}$$

Compared with hard saturation, this formulation is continuously differentiable and is therefore more suitable for numerical integration and gain-scheduling implementations.

To reduce integrator windup during saturation, a conditional anti-windup mechanism is included in the augmented dynamics. In particular, the integration of the tracking error is suspended when the magnitude of the control signal exceeds a predefined threshold close to the actuator limit, selected here as 95% of v_{max}.

IV. Simulation Setup and Results

Both controllers were evaluated in a discrete-time simulation environment with a sampling frequency of 250 Hz and a total simulation duration of 50 s. For a fair comparison, the SDRE and SA controllers were tested on the same nonlinear plant model, with the same sampling period, actuator saturation, anti-windup mechanism, and disturbance injection within each scenario. In both scenarios, the control inputs were limited through the smooth saturation law with $v_{max} = 5$ V, and the integral states were updated only when the commanded voltages remained below 95% of the actuator limit. All simulations were performed in MATLAB R2025a on a 64-bit Windows laptop equipped with an Intel Core i5-1240P CPU at 1.70 GHz and 8 GB RAM. The CPU times reported in the tables were obtained on the same workstation and are therefore used as relative computational indicators rather than hardware-independent real-time guarantees.

The input weighting matrix was kept fixed as $R = \mathrm{diag}(0.5, 0.5)$, whereas the state weighting matrix Q was selected separately for each scenario through heuristic tuning. Therefore, the reported Q matrices are scenario-specific and should not be interpreted as a single globally tuned weighting matrix for all simulation cases.

A. Scenario 1: Step Tracking Under Severe Wind Gust

For this scenario, the reference inputs were 35° for elevation and 60° for travel, both applied at $t = 5$ s. The weighting matrix was $Q = \mathrm{diag}([40,\ 5,\ 5,\ 1,\ 10,\ 15,\ 1,\ 1,\ 4,\ 2])$, with $R = \mathrm{diag}(0.5,\ 0.5)$. To evaluate disturbance rejection, an asymmetric wind-gust input $u_{dist} = [3.5,\ -3.5]^T$ was applied over the interval $25 \le t \le 28$ s.

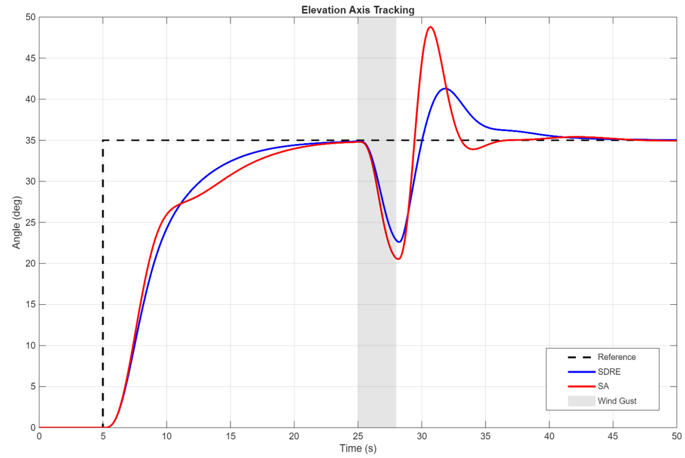

Fig. 3. Elevation tracking in Scenario 1.

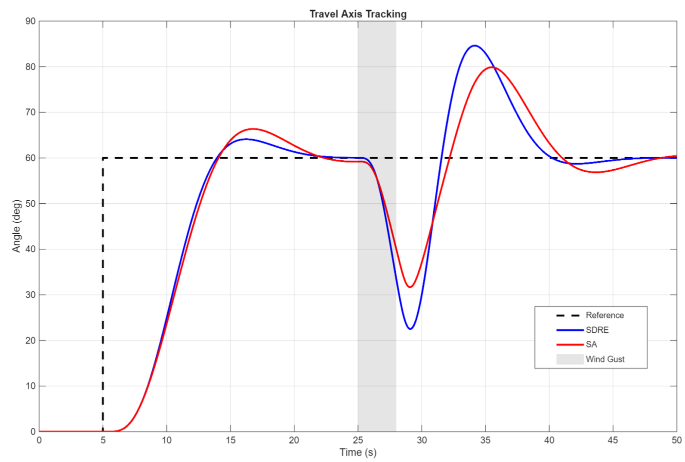

Fig. 4. Travel tracking in Scenario 1.

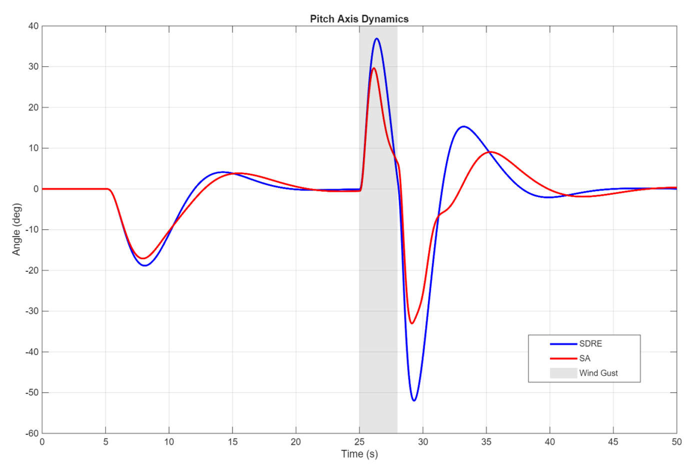

Fig. 5. Pitch response in Scenario 1.

As illustrated in Figs. 3 and 4, both controllers successfully regulated the system to the desired setpoints. When the wind gust was applied, both SDRE and SA experienced transient deviations but recovered after the disturbance interval. Because the system remained relatively close to a mildly nonlinear operating region after the step transition,

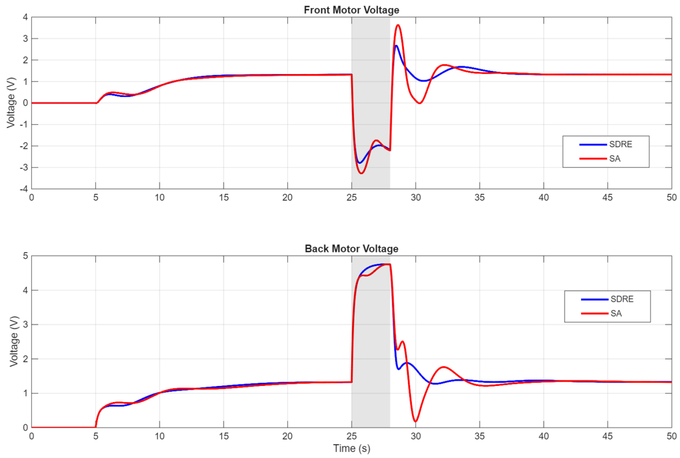

Fig. 6. Control voltages in Scenario 1.

TABLE II
QUANTITATIVE PERFORMANCE METRICS (SCENARIO 1 - STEP & WIND)

Metric	SDRE Controller	SA Controller
CPU Time (s)	20.31	20.85
Total Cost (J)	2510.45	2502.12

the local Jacobian-based approximation used by the SA controller remained sufficiently accurate to preserve acceptable tracking performance. This explains why the performance gap between the two methods is limited in Scenario 1.

B. Scenario 2: 3D Spiral Tracking with Wind Gust

Scenario 2 was designed to evaluate both methods under sustained nonlinear motion. In this case, the system was required to follow a highly coupled three-dimensional spiral trajectory, which kept the states in a continuous transient regime throughout the simulation.

The reference signals were defined as

$$\theta_{ref}(t) = \frac{45^\circ}{50}t, \qquad \psi_{ref}(t) = \frac{4\pi}{50}t, \qquad 0 \le t \le 50 \text{ s},$$

which corresponds to a climbing three-dimensional spiral motion over the simulation interval. For this case, the weighting matrix was chosen as

$$Q = \text{diag}([50,\ 5,\ 5,\ 1,\ 10,\ 20,\ 1,\ 1,\ 4,\ 2]).$$

An asymmetric wind-gust input

$$u_{dist} = [1.0,\ -1.0]^T$$

was applied during the interval $25 \le t \le 28$ s.

As shown in Fig. 7 and Fig. 8, the difference between the two controllers becomes more pronounced in this scenario. Since the helicopter remains in a continuously changing operating condition, the local linearization used by the SA controller becomes less reliable as the maneuver progresses and the disturbance is introduced. Consequently, the SA controller exhibits larger oscillations and more visible degradation in tracking performance, whereas the SDRE controller maintains smoother responses by preserving the state-dependent structure of the nonlinear model..

The control profiles in Fig. 9 further support this observation. During the disturbed interval, the SA controller drives

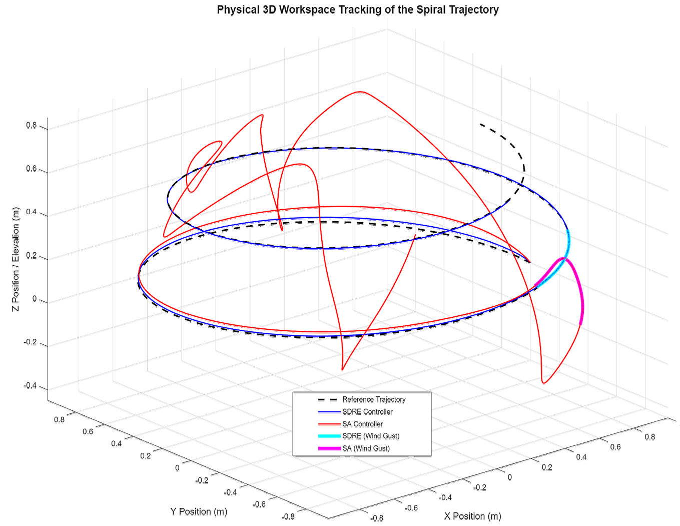

Fig. 7. 3D workspace tracking in Scenario 2.

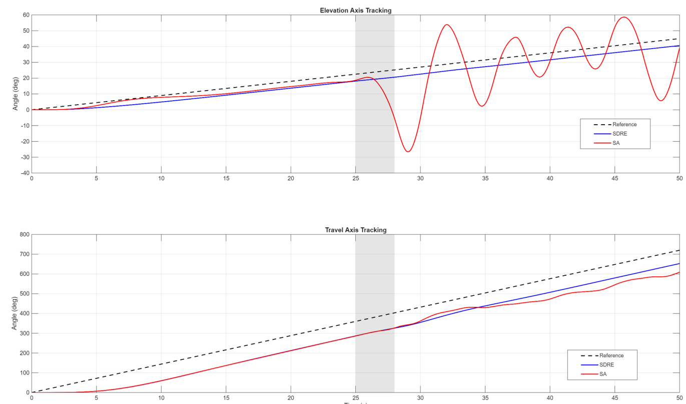

Fig. 8. Elevation and travel tracking in Scenario 2.

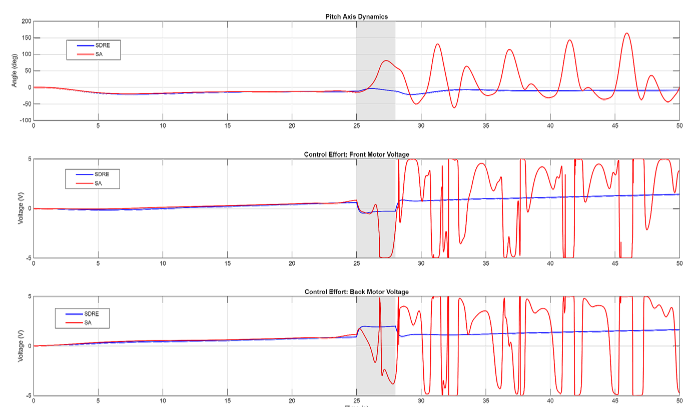

Fig. 9. Pitch response and front/back motor voltages in Scenario 2.

the motor voltages closer to the saturation limits and exhibits more oscillatory compensation behavior, whereas the SDRE controller produces a smoother response while maintaining better trajectory tracking.

A comparison of Table III indicates that the quadratic cost J alone does not fully reflect trajectory-tracking quality in this scenario. A controller may yield a lower cost by using less control effort even when its tracking performance is poorer over a prolonged interval. For this reason, the ITAE and ITSE metrics provide a more informative basis for

TABLE III
QUANTITATIVE PERFORMANCE METRICS (SCENARIO 2 - SPIRAL TRACKING & WIND GUST)

Metric	SDRE Controller	SA Controller
CPU Time (s)	20.62	20.91
Total Cost (J)	66767.20	56839.26
ITAE	1643.62	2145.02
ITSE	1939.41	3040.83

comparison. In particular, the larger ITSE value obtained by the SA controller is consistent with the sustained oscillatory behavior observed after disturbance injection.

Overall, the results of Scenario 2 indicate that, for the selected spiral reference, weights, and wind-gust profile, the SDRE controller provides more reliable tracking performance than the implemented SA controller.

V. CONCLUSION

This paper compared SDRE and SA controllers for trajectory tracking of a nonlinear 3-DOF helicopter under two scenarios: step tracking and three-dimensional spiral tracking with wind disturbance. The results showed that both methods performed satisfactorily in the nominal step-tracking case, whereas the SDRE controller provided smoother responses and better tracking performance in the more demanding spiral maneuver.

The observed difference can be attributed to the fact that SDRE preserves the state-dependent nonlinear structure of the plant, while SA relies on repeated local linearization. Under the considered operating conditions, this led to larger oscillations and higher time-weighted tracking errors for the SA controller during the disturbed spiral trajectory.

Overall, the results indicate that SDRE is the more reliable option for the specific nonlinear helicopter benchmark, weighting matrices, reference profiles, and wind disturbances considered in this study. A broader conclusion would require additional references, tunings, and fully nonlinear controllers such as backstepping or exact feedback linearization, which are planned as future extensions.

REFERENCES

[1] T. Cimen, "State-dependent Riccati equation (SDRE) control: A survey," *IFAC Proceedings Volumes*, vol. 41, no. 2, pp. 3761-3775, 2008.

[2] J. R. Cloutier, "State-dependent Riccati equation techniques: an overview," in *Proc. of the 1997 American Control Conference*, vol. 2, pp. 932-936, 1997.

[3] A. C. Arican, S. Ozcan, B. M. Kocagil, U. M. Guzey, E. H. Copur, and M. U. Salamci, "Linear and nonlinear optimal controller design for a 3 DOF helicopter," in *Proc. 2018 19th International Carpathian Control Conference (ICCC)*, 2018.

[4] A. C. Arican, S. Ozcan, B. M. Kocagil, U. M. Guzey, and M. U. Salamci, "Suboptimal control of a 3 DOF helicopter with state dependent Riccati equations," in *Proc. 2017 XXVI International Conference on Information, Communication and Automation Technologies (ICAT)*, 2017.

[5] E. H. Copur, A. C. Arican, S. Ozcan, and M. U. Salamci, "An update algorithm design using moving Region of Attraction for SDRE based control law," *Journal of the Franklin Institute*, vol. 356, no. 15, pp. 8388-8413, 2019.

[6] A. Redzovic and A. Tahirovic, "State estimation and control for continuous-time nonlinear systems: A unified SDRE-based approach," in *Proc. 2025 IEEE International Conference on Control, Decision and Information Technologies (CoDIT)*, 2025.

[7] A. Di Biase, S. Longhi, and A. Bonci, "Closed-form SDRE control solution for second-order non-linear systems," in *Proc. 2025 IEEE 64th Conference on Decision and Control (CDC)*, 2025.

[8] H. Ghadiri, A. Mohammadi, and H. Khodadadi, "Fast terminal sliding mode control based on SDRE observer for two-axis gimbal with external disturbances," *Journal of the Brazilian Society of Mechanical Sciences and Engineering*, vol. 44, pp. 70, 2022.

[9] S. R. Nekoo and A. Ollero, "Experimental implementation of state-dependent Riccati equation control on quadrotors," *Drone Systems and Applications*, vol. 13, pp.1-16, 2025.

[10] L. Saluzzi, "The State-Dependent Riccati Equation in Nonlinear Optimal Control: Analysis and Numerical Approximation," *Journal of Optimization Theory and Applications*, vol. 209, no. 1, pp. 34, 2026.

[11] A. Gonzalez-Morgado, S. R. Nekoo, G. Heredia, and A. Ollero, "Bidirectional-thruster multirotor for perimeter pipe inspections (BiMPPI): A nonlinear optimal integral-SDRE design," *ISA Transactions*, vol. 161, pp. 276-288, 2025.

[12] A. D. Ogundele, "Nonlinear optimal controller design for nonlinear spacecraft formation flying with periodic coefficients via SDRE technique," *Aerospace Systems*, vol. 5, pp. 247-263, 2022.

[13] B. Li, X. Gao, H. Huang, and H. Yang, "Nonlinear trajectory tracking control of underactuated AUVs using the state-dependent Riccati equation (SDRE) with parameter perturbation," *Nonlinear Dynamics*, vol. 111, pp. 18027-18041, 2023.

[14] S. K. Mitter, "Successive approximation methods for the solution of optimal control problems," *Automatica*, vol. 3, no. 3-4, pp. 135-149, 1966.

[15] K. A. Wise and J. L. Sedwick, "Successive approximation solution of the HJI equation," in *Proc. of the 33rd IEEE Conf. on Decision and Control*, vol. 2, pp. 1387-1391, 1994.

[16] R. W. Beard, "Successive Galerkin approximation algorithms for nonlinear optimal and robust control," *International Journal of Control*, vol. 71, no. 5, pp. 717-743, 1998.

[17] I. Maruta, S. Nishida, and K. Fujimoto, "A study on numerical solutions of Hamilton-Jacobi-Bellman equations based on successive approximation approach," *SICE Journal of Control, Measurement, and System Integration*, vol. 13, no. 3, pp. 157-163, 2020.

[18] Z. Wang, S. Niu, and L. Li, "Sparse successive approximation for nonlinear H_2 and H_∞ optimal control problems under residual errors," *ISA Transactions*, vol. 145, pp. 63-77, 2024.

[19] Z. Aganovic and Z. Gajic, "The successive approximation procedure for finite-time optimal control of bilinear systems," *IEEE Transactions on Automatic Control*, vol. 39, no. 9, pp. 1932-1935, 1994.

[20] H. Jaddu and M. Vlach, "Successive approximation method for nonlinear optimal control problems with application to a container crane problem," *Optimal Control Applications and Methods*, vol. 23, no. 5, pp. 275-288, 2002.

[21] Y. Liu, Y. Zhou, and Y. Zhang, "A successive approximation approach for stochastic systems with state delay and multiplicative noise in the blast furnace process," in *Proc. 37th Chinese Control and Decision Conference (CCDC)*, 2025.

[22] J.-S. Ha, J.-J. Lee, and H.-L. Choi, "A successive approximation-based approach for optimal kinodynamic motion planning with nonlinear differential constraints," in *Proc. 52nd IEEE Conf. on Decision and Control (CDC)*, pp. 3623-3628, 2013.

[23] N. Babaei and M. U. Salamci, "Controller design for personalized drug administration in cancer therapy: Successive approximation approach," *Optimal Control Applications and Methods*, vol. 39, no. 2, pp. 682-719, 2018.

[24] Z. Wang and Y. Li, "Rigid spacecraft nonlinear robust H_∞ attitude controller design under actuator misalignments," *Nonlinear Dynamics*, vol. 111, no. 16, pp. 15037-15054, 2023.

[25] G.-Y. Tang and H.-H. Wang, "Successive approximation approach of optimal control for nonlinear discrete-time systems," *International Journal of Systems Science*, vol. 36, no. 3, pp. 153-161, 2005.

[26] S. Elloumi, B. Abidi, and N. B. Braiek, "Decentralized optimal controller design for multimachine power systems using successive approximation approach," *Journal of the Franklin Institute*, vol. 350, no. 10, pp. 2994-3010, 2013.